

Nonmonotonous evolution of the Kondo temperature in the phase diagram of $\text{Ce}(\text{Pd}_{1-x}\text{Cu}_x)_2\text{Si}_2$

M. Gomez Berisso, O. Trovarelli, and P. Pedrazzini

Div. Bajas Temperaturas, Centro Atómico Bariloche (CNEA), 8400 S.C. de Bariloche, Argentina

G. Zwicknagl

Max-Planck-Institut für Physik komplexer Systeme, Außenstelle Stuttgart, Postfach 80 06 65, 70506 Stuttgart, Germany

C. Geibel and F. Steglich

Max-Planck-Institut für Chemische Physik fester Stoffe, D-01187 Dresden, Germany

J. G. Sereni

Div. Bajas Temperaturas, Centro Atómico Bariloche (CNEA), 8400 S.C. de Bariloche, Argentina

(Received 29 August 1997)

The evolution of the behavior of the Ce $4f$ electron with the Cu content in the alloy $\text{Ce}(\text{Pd}_{1-x}\text{Cu}_x)_2\text{Si}_2$ was investigated by determining its structural, magnetic, transport, and thermal properties. Results obtained on 15 samples with compositions distributed along the whole concentration range allow us to draw a magnetic phase diagram showing three distinct regions. The first region at low Cu concentrations corresponds to the antiferromagnetic-ordered regime. The fast suppression of this magnetic order between $x=0.2$ and $x=0.25$ suggests the presence of a critical point which separates this region from the second one at larger x values where no magnetic order is observed. The main characteristic of this second region, which extends up to $x=0.7$, is a pronounced increase of the Kondo temperature T_K , from $T_K \approx 15$ K at $x=0.25$ to $T_K \approx 50$ K at $x=0.7$. This is in contrast with the fast decrease of T_K in the region with $x > 0.7$. In this region a small anomaly with a ferromagnetic character is observed in the specific heat around 4 K. The change in the evolution of T_K with x coincides with a change in the composition dependence of the c lattice parameter of the tetragonal structure, pointing to a structure-related origin of this unusual $T_K(x)$ behavior. This nonmonotonous $T_K(x)$ dependence is reproduced using local-density-approximation band-structure calculations, which show a maximum of the hybridization strength between conduction electrons and Ce $4f$ states for intermediate Cu concentrations. Such a $T_K(x)$ dependence which contradicts the monotonous dependence observed in all other Ce-based alloy systems is the hallmark of the $\text{Ce}(\text{Pd}_{1-x}\text{Cu}_x)_2\text{Si}_2$ alloy, which cannot be described as a Fermi-liquid system in the nonmagnetic region. [S0163-1829(98)02118-3]

I. INTRODUCTION

Among the Ce ternary compounds, the family of the $\text{Ce}T_2X_2$ intermetallics (where T is a transition or noble metal and X a p -type metalloid) shows one of the richest varieties of behaviors within a single type of crystalline structure (i.e., ThCr_2Si_2). In this group, the largest modification in the physical properties is obtained by changing the T element, which from size and electronic structure drives significant changes in the Fermi surface of the system. Those effects are directly reflected in the “Ce- T ” and “Ce- X ” interatomic distances, allowing a systematic description of all the members of this family of compounds in terms of the Ce-ligand spacing.^{1,2} With the exception of the ferromagnetic (F) compound CeRu_2Ge_2 (Ref. 3) different types of antiferromagnetic (AF) structures and interactions were found in this group. Some of the most interesting examples are CeRh_2Si_2 (Ref. 3) with the highest AF transition for a Ce system (a Néel temperature of $T_N=35$ K), CePd_2Si_2 with $T_N=10$ K,³ similar to that of its isotypic GdPd_2Si_2 ,³ in clear disagreement with the de Gennes factor proportionality, and $\text{CeCu}_{2-x}\text{Si}_{2+x}$,⁴ in which magnetic order with fluctuating moments competing with superconductivity (SC) has been observed. Within the nonmagnetic members of this family,

normal [CeRu_2Si_2 , (Ref. 5)] and SC [$\text{CeCu}_{2+x}\text{Si}_{2-x}$ (Refs. 6,7)] heavy fermions were found. At the limit of strong $4f$ -band hybridization, some representative compounds of intermediate valence behavior were observed, such as, for example, CeNi_2P_2 , which shows the lowest density of states and the shortest Ce- X distance.⁸

A common feature of the mentioned compounds is that a small reduction in their respective interatomic distances strongly enhances the Ce-ligand electronic overlap, with a consequent hybridization enhancement. Therefore, those compounds located at the limit of Ce-ligand contact [mainly “Ce- X ” (Ref. 2)] are at the verge of a magnetic instability, as evidenced by drastic changes under pressure and alloying. For example, three AF compounds, CeRh_2Si_2 , CePd_2Si_2 , and CeCu_2Ge_2 , become SC under a pressure $P=0.9$ GPa,⁹ 2.9 GPa,¹⁰ and 7 GPa,¹¹ respectively. The corresponding decrease of the ordering temperature ($\Delta T_N/\Delta P$) results in being strong for CeRh_2Si_2 [$\Delta T_N/\Delta P = -38$ K/GPa (Ref. 9)], moderate for CePd_2Si_2 [$\Delta T_N/\Delta P = -3.4$ K/GPa (Ref. 10)], and weak for CeCu_2Ge_2 [$\Delta T_N/\Delta P = -0.6$ K/GPa (Ref. 11)]. Concerning the ligand concentration dependence, $\text{CeCu}_{2+x}\text{Si}_{2-x}$ is a prototype for alloying effects because some percentual variation of stoichiometry produces drastic changes in the ground state that include magnetic, nonmag-

netic, and SC behaviors.^{6,7} On the other hand, these variations can be compensated by some tenth of GPa of applied pressure.^{5,12} The smallness of the changes in the driving parameters gives an idea of the low-energy scale involved in the transition between the different ground states in these compounds.

Another striking behavior observed in this family of compounds is the presence of a non-Fermi-liquid (NFL) phase at the boundary of the SC phase, which transforms to a Fermi-liquid (FL) phase under strong magnetic fields.¹² This NFL behavior, extracted from the linear temperature dependence of the electrical resistivity, is observed in the SC phase of CePd₂Si₂ under pressure,¹⁰ whereas deviations from linearity were found in the pressure-induced SC phases of CeRh₂Si₂ (Ref. 9) and CeCu₂Ge₂ (Ref. 11).

By alloying, either volume or electronic density modifications can be induced in the system depending on the relative size and electronic structure of the substitutes, inducing different types of magnetic phase diagrams.¹³ In the case of Ce(Pd_{1-x}Cu_x)₂Si₂,¹⁴ both variations are driven as Cu replaces Pd, although the opposite effect is expected with respect to the hybridization strength because Cu doping reduces the volume whereas it increases the number of electrons. Previous studies on this system¹⁴ revealed a rapid decrease of T_N with Cu concentration, and an unusual reduction of the $C_{el}(T)/T \rightarrow 0$ ratio of the electronic specific heat at intermediate Pd substitution related to a significant reduction of the entropy gain. Such a minimum of $C_{el}(T)/T \rightarrow 0$ is quite unusual because the systems undergoing a magnetic-ordered to nonmagnetic transformation by alloying show just the contrary, i.e., a maximum in $C_{el}(T)/T$ as a function of x before becoming intermediate valent.¹⁵ Furthermore, the system at hand does not evolve to an intermediate valent state, but on the contrary enhances its heavy fermion character as $x \rightarrow 1$.

The aim of this work is to build up a detailed phase diagram of the Ce(Pd_{1-x}Cu_x)₂Si₂ system based on structural, transport, magnetic, and thermal measurements. For such a purpose we have extended the aforementioned study to a much larger number of samples and range of temperatures, particularly at the critical concentrations where the ordering temperature vanishes and the c -axis dependence with concentration changes its slope.

II. EXPERIMENTAL DETAILS AND RESULTS

Samples with concentrations $x=0, 0.05, 0.1, 0.2, 0.25, 0.3, 0.4, 0.5, 0.6, 0.7, 0.8, 0.85, 0.9,$ and 1 were prepared by arc melting the appropriate amount of pure metals in an argon atmosphere. This procedure was repeated several times in order to homogenize the sample composition. After that, the samples were annealed 120 h between 700 and 1000 °C. Powder x-ray diffractometry confirmed that the samples were single phase with tetragonal ThCr₂Si₂ structure within the resolution of the technique (≈ 2 at. %).

Specific heat measurements were performed in a ³He quasiadiabatic calorimeter by the usual pulse technique between 0.4 and 25 K and in some cases applied magnetic field up to $B=4$ T. In order to extract the electronic contribution C_{el} to the total specific heat we measured isotopic La compounds, La(Pd_{1-x}Cu_x)₂Si₂, for $x=0, 0.6,$ and $1,$ and per-

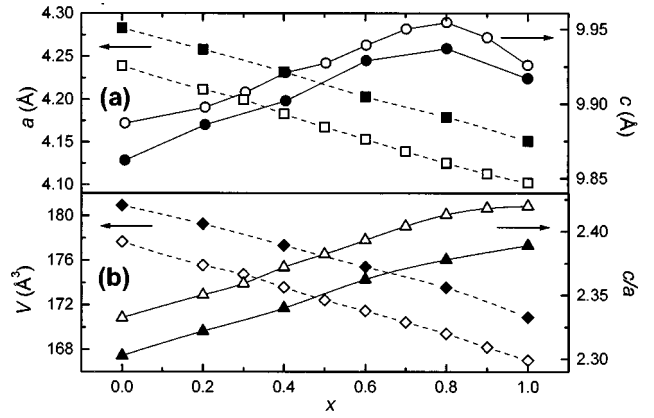


FIG. 1. Concentration dependence of (a) the lattice parameters and (b) volume and c/a ratio of Ce(Pd_{1-x}Cu_x)₂Si₂ (open symbols) and La(Pd_{1-x}Cu_x)₂Si₂ (solid symbols).

formed a linear interpolation for concentrations in between.

The magnetic dc susceptibility was measured between 1.8 K and 300 K in a commercial superconducting quantum interference device (SQUID) magnetometer under a field of $B=0.1$ T. Some samples were studied using ac magnetic susceptibility between 0.4 and 20 K with a mutual-inductance bridge working at a fixed frequency of 128 Hz.

Electrical resistivity was measured with a conventional four-contact technique with lock-in detection on planar samples for temperatures between 0.45 K and 300 K in a ³He cryostat. In order to avoid the uncertainties related to the geometric factor of the samples, we have normalized the results to the resistance value at 300 K.

Figure 1 shows the composition dependence of the a and c lattice parameters, of the ratio c/a , and of the unit-cell volume of Ce(Pd_{1-x}Cu_x)₂Si₂, together with the non- f reference alloy La(Pd_{1-x}Cu_x)₂Si₂. Both systems present the same behavior, characterized by a clear difference between the evolution of the a and c parameters with x [see Fig. 1(a)]. Whereas the a axis decreases almost linearly the c axis increases slightly at low Cu contents and decreases at large Cu contents, presenting a clear change of slope at $x=0.8$. Because the change of the relative change of the a axis is nearly one order of magnitude larger than that of the c axis, the unit-cell volume decreases monotonously from the Pd-rich to the Cu-rich side with only a small change in the slope at $x \approx 0.8$ [see Fig. 1(b)]. The difference of volume between La- and Ce-based compounds is approximately 1.7%, independently of x . The c/a ratio increases with x until $x=0.7$, and then tends to saturate at the value $c/a=2.419$ for CeCu₂Si₂ (Ref. 14) and $c/a=2.389$ for LaCu₂Si₂, respectively.

The temperature dependence of the electrical resistivity, $\rho(T)$, gives a first idea about the peculiar evolution of the physical properties of this alloy. Figure 2 shows the ratio $\rho(T)/\rho(300\text{ K})$ in the temperature range $4\text{ K} < T < 300\text{ K}$ for selected samples across the whole composition range. For low Cu contents, $\rho(T)$ presents a well-defined maximum at low temperatures ($T \approx 10-20$ K) and a weak bump around 80 K. The low-temperature maximum shifts to higher temperatures with increasing x . As a result both features almost merge at $x=0.8$, making their distinction difficult. However, for $x > 0.8$, the low-temperature maximum shifts back to

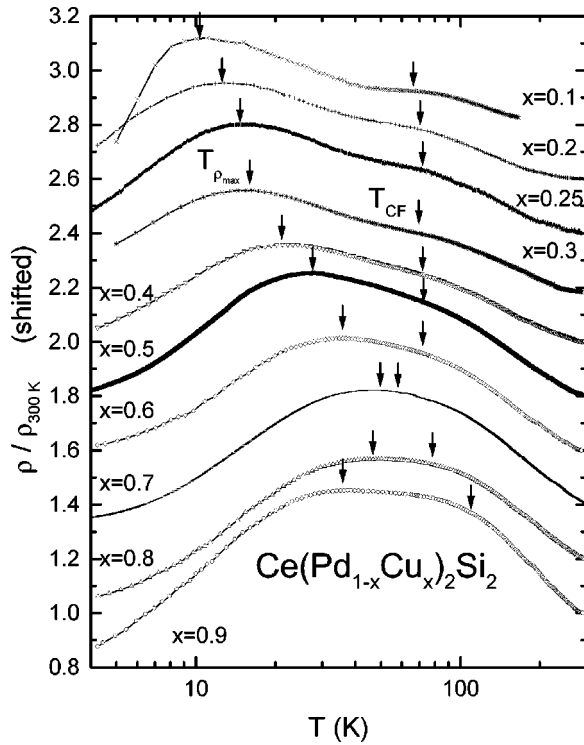


FIG. 2. Electrical resistivity normalized to its room temperature value vs $\ln(T)$. The arrows mark the position of $T_{\rho_{\max}}$ and T_{CF} (see text). The curves are shifted along the ρ axis for clarity.

lower temperatures. From a comparison with the well-known properties of the pure compounds, the low-temperature maximum and the anomaly at high temperature are connected with the Kondo scattering of the crystal-electric-field (CF) ground state and excited doublet, respectively. Thus, to our knowledge, these results of the electrical resistivity give clear evidence for a nonmonotonous evolution of the Kondo temperature in Ce compounds.

The dc susceptibility $\chi_{dc}(T)$ of CePd_2Si_2 shows a clear kink at $T_N=10.3$ K related to the AF transition. Substitution of Pd by Cu reduces T_N and smears out the transition (see Fig. 3), which can no longer be resolved for $x>0.2$. Instead

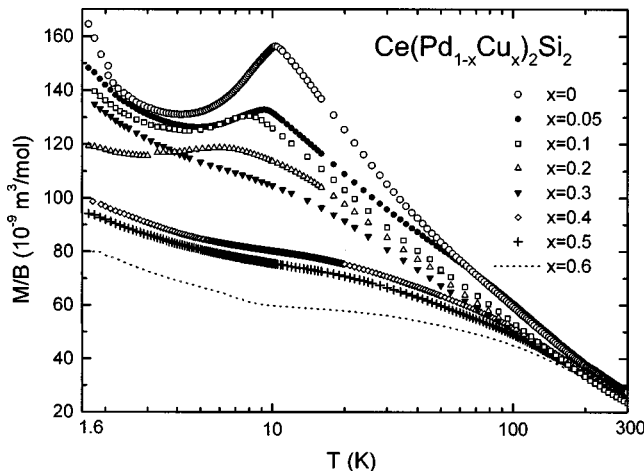


FIG. 3. dc magnetic susceptibility of the Pd-rich concentration region in a semilogarithmic representation. The sample $x=0.85$ is enriched in the T -metal concentration (see text).

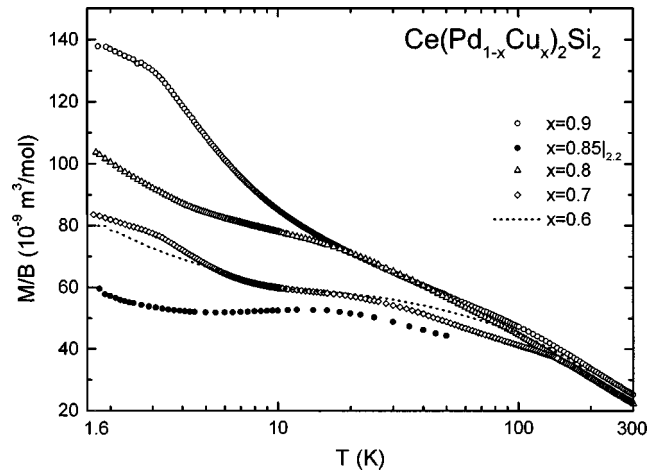


FIG. 4. dc magnetic susceptibility of the Cu-rich concentration region in a semilogarithmic representation.

the temperature dependence of $\chi_{dc}(T)$ gets quite flat below 20 K, leading to a broad inflection which shifts to higher temperatures with increasing x . In the $x=0.6$ sample, a weak but clear F contribution appears below $T=7$ K. For $x>0.6$, the susceptibility below 40 K increases again with Cu concentration, and the F contribution gets larger (Fig. 4). However, this F contribution turned out to be sample dependent. Since the foreign phase formed during the peritectic reaction of the Cu-rich samples presents such a F signal,¹⁶ a further sample with composition $\text{Ce}(\text{Pd}_{0.15}\text{Cu}_{0.85})_{2.2}\text{Si}_2$ was prepared and investigated. Such a transition-metal excess is known to strongly reduce the amount of this foreign phase. No F contribution was detected in the $\chi_{dc}(T)$ measurement performed on this sample, indicating that this contribution to the magnetic signal is not intrinsic, and it can be accounted for by less than 2% of foreign phase.

The evolution of the ground state with composition can be followed in more detail in the specific heat measurements. In Fig. 5, C_{el}/T is plotted as a function of T for the Pd-rich samples. CePd_2Si_2 presents a sharp mean-field-type transition at $T_N=10.3$ K and a second small anomaly at $T_m=7.8$ K. With increasing x , both anomalies shift to lower tempera-

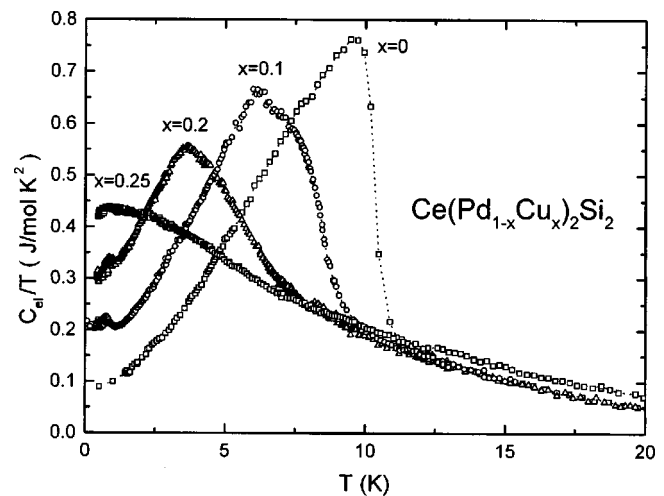


FIG. 5. $C_{el}(T)/T$ vs T for the magnetically ordered samples. The nonmagnetic sample $x=0.25$ is included for comparison.

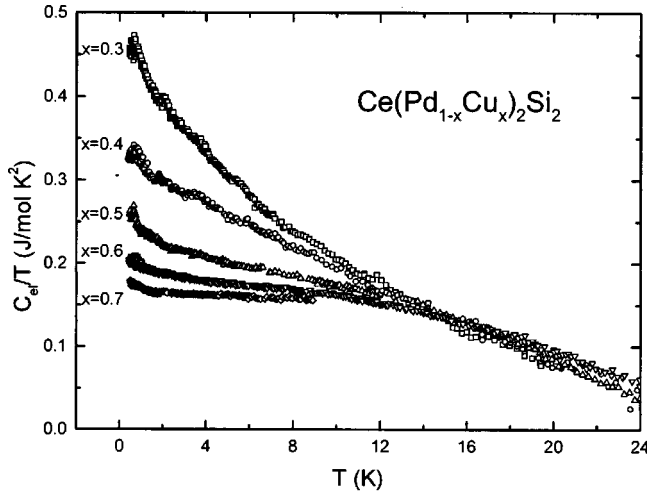


FIG. 6. $C_{el}(T)/T$ vs T for the samples with intermediate concentrations. For clarity, the data of $x=0.7$ sample is included up to 9 K only.

tures and the $C_{el}(T)$ jump at T_N becomes broader, whereas the anomaly at T_m becomes more pronounced, transforming into a well-defined peak in $C_{el}(T)/T$. The distinction between T_N and T_m in the $x=0.05$, 0.1 , and 0.2 samples is more evident in a $\partial(\chi T)/\partial T$ versus T plot (not shown here) where a clear break in the slope is observed at T_m . Thus, T_m is probably related to a transition between different AF structures. For $x=0.25$ no transition can be resolved. A closer inspection of the low-temperature region shows a further anomaly at $T_0 \approx 0.8$ K for the samples with $x=0.1$ and 0.2 . This anomaly only involves a few degrees of freedom. In spite of that, the $\chi_{ac}(T)$ measurement performed on the $x=0.2$ sample shows a stronger signal at $T=T_0$ than that observed at T_m .

For the intermediate Cu concentration range $0.3 \leq x \leq 0.7$ (see Fig. 6), $C_{el}(T)/T$ increases monotonously as temperature decreases and no anomalies are observed above 0.4 K. The slope of $C_{el}(T)/T$ versus T decreases with x and thus the Sommerfeld coefficient $\gamma_0 = C_{el}(T)/T|_{T \rightarrow 0}$ decreases from 0.5 J/mol K² for $x=0.3$ to 0.16 J/mol K² for $x=0.7$. In the high Cu concentration region $0.7 < x \leq 1$, γ_0 grows again monotonously with x . A broad maximum is observed in $C_{el}(T)/T$ at 4 K for $x=0.8$ and 0.85 , but it can also be observed as a shoulder in the $x=0.9$ sample. For the analysis of the $x \rightarrow 1$ region we chose to compare the results with those of a CeCu₂Si₂ ‘‘A-phase’’ sample, where the magnetic ‘‘A phase’’ and SC phase were suppressed by applying a small amount of external pressure and magnetic field [the corresponding curve is labeled ‘‘N’’ in Fig. 7 (Ref. 17)]. This corresponds to a system with a slightly larger hybridization strength and without a phase transition, which is thus very close to the situation of the Cu-rich samples. A compilation of characteristic properties extracted from the resistivity, susceptibility, and specific heat results is given in Table I.

III. DISCUSSION

From these results, it is clear that the evolution of the Ce(Pd_{1-x}Cu_x)₂Si₂ system with concentration can be divided

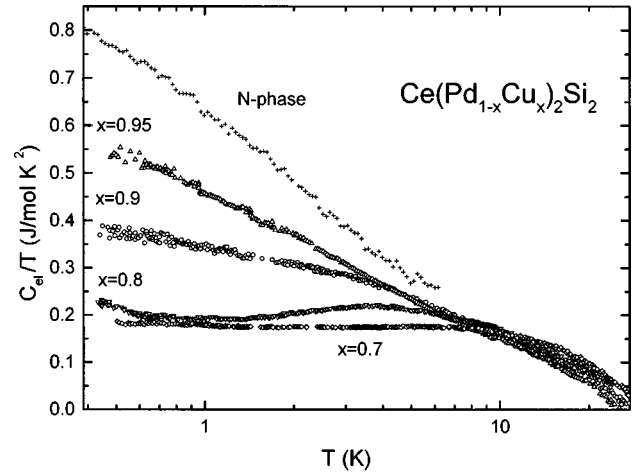


FIG. 7. $C_{el}(T)/T$ vs T for the Cu-rich samples. The characteristic of the CeCu₂Si₂ sample labeled as ‘‘N-phase’’ are given in the text.

into three regions. The Pd-rich side presents an AF-ordered phase with an ordering temperature that decreases with Cu content. The intermediate region $0.3 \leq x \leq 0.7$ is characterized by the lack of long-range magnetic order (LRMO) and the increase of the Kondo temperature (T_K) with x . Such a concentration dependence of $T_K(x)$ marks the difference with the Cu-rich side ($x > 0.8$) where T_K decreases with x from about 50 K to 10 K for CeCu₂Si₂.¹⁴

On the Pd-rich side, the AF phase seems to disappear rather abruptly between $x=0.2$ and $x=0.25$. A more detailed

TABLE I. Values of T_N and T_m [K]; n , exponent of $\rho \sim T^n$; χ at 10 K [10^{-9} m³/mol]; $\gamma_0 = C_{el}(T)/T|_{T \rightarrow 0}$ [J/mol K²]; ΔS , normalized entropy $\Delta S(20K)/R \ln 2$; T_{CF} , position of the CF-related maximum of $\rho(T)$ [K]; and T_K , Kondo temperature [K].

x	T_N (T_m)	n	χ_{10K}	γ_0 (ΔS)	T_{CF}	T_K
0.0	10.3 (7.7)	2.5 ^a	156	0.12 (0.9)	70	
0.05	9.4 (7.3)		132			
0.1	8.4 (6.4)	(1.65) ^b 2.4	127	0.20 (0.87) ^f	67	13.8
0.2	5.5 (3.5)	(2.4) ^c 2.0	113	0.4 (0.82) ^f	71	15
0.3		1.25	105	0.5 (0.78) ^f	68	16
0.4		1.45	82	0.29 (0.66)	73	23
0.5		1.67	75	0.19 (0.60)	77	26
0.6		(2.0) ^d 1.62	60	0.17 (0.53)	77	41
0.7		1.68	60	0.16 (0.54)	68	49
0.8		2.3		0.19 (0.58)	80	50
0.9				0.40 (0.64)		
0.95				0.57 (0.64)	110	34
1.0		2.0 ^e		0.8 (0.78)	150 ^g	

^aAfter Ref. 11.

^bBelow $T \sim 3.6$ K.

^cBelow $T \sim 1.7$ K.

^dBelow $T \sim 1.6$ K.

^eA/S sample (after Ref. 7).

^fExtrapolated from $T \sim 15$ K.

^gAfter Ref. 23.

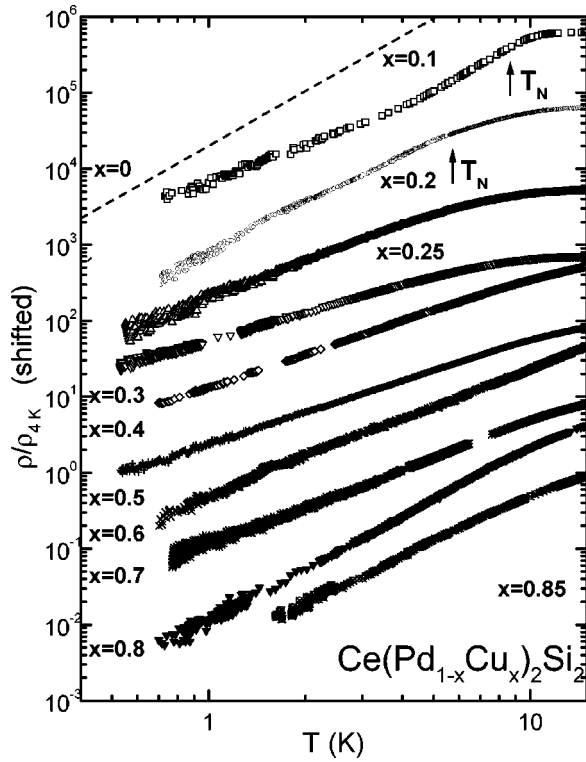


FIG. 8. Normalized low-temperature electrical resistivity vs temperature in a double-logarithmic scale to show the different power laws of $\rho \propto T^n$.

analysis of the specific heat results reveals that the entropy associated with the magnetic order decreases more rapidly than T_N and tends to zero within this range of concentration. This might suggest a critical point in the range $0.2 < x < 0.25$.

We have to remark that the tail of $C_{el}(T)/T$ above T_N is almost independent of concentration up to $x=0.2$ (see Fig. 5) and increases only slightly for $x=0.25$, indicating that the significant magnetic fluctuations present in the paramagnetic phase are practically not affected by Cu doping. This suggests that the magnetic excitations are not quenched in the same way as the LRMO but that they survive the LRMO disappearance. Since the slope of $C_{el}(T)/T$ below T_m is also similar for the samples with $x \leq 0.2$, neither the magnon dispersion relation (below T_m) changes with Cu concentration.

The disappearance of the magnetic order is accompanied by a drastic change in the exponent n of the power law fits to $\rho(T)$ (see Fig. 8). In the AF-ordered regime, one observes rather large values of n : starting from $n=2.5$ at $x=0$.¹¹ For $x=0.1$ a $T^{2.4}$ dependence is found for $T > T_N/2$ and $T^{1.65}$ for $T < T_N/2$, whereas for $x=0.2$ T^2 is observed for $T > T_N/2$ and a $T^{2.4}$ dependence is found for $T < T_N/2$.

In contrast, for $x=0.3$ where the AF ordering has disappeared, n drops to $n=1.25$, which is the lowest value observed for the whole alloy system. Such a low exponent value is taken as the hallmark for NFL behavior.¹⁸ In fact, for those concentrations neither $C_{el}(T)/T$ nor $\chi(T)$ can be described as FL systems, where these parameters are expected to become constant for $T \rightarrow 0$ with $C_{el}(T)/T \sim \chi \sim \sqrt{A}$, being A the coefficient of the $\rho = AT^2$ law. For higher x values, n increases slowly up to $n=1.62$ for $x=0.7$.

As quoted above, the intermediate concentration region

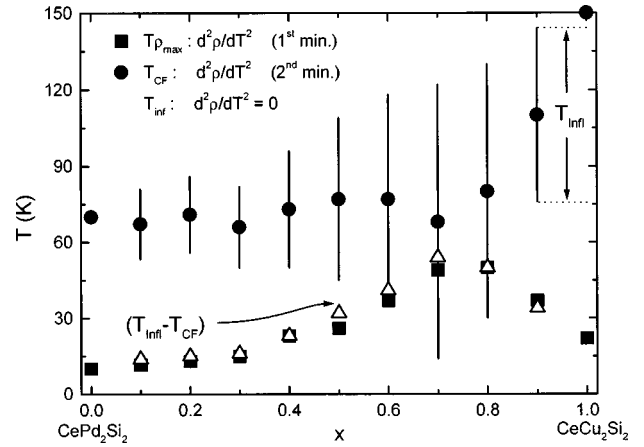


FIG. 9. Phase diagram of the high-temperature parameters extracted from $\rho(T)$ (see text). $T_{\rho_{\max}}$ is the temperature where the first minimum of $d^2\rho/dT^2$ occurs which is related to the Kondo temperature. T_{CF} is the temperature where the second minimum of $d^2\rho/dT^2$ occurs which is related to the crystal field splitting. The $\rho(T)$ inflection point T_{inf} is associated with the hybridization of the first excited CF levels Γ_{CF} through the relation $\Gamma_{CF} = T_{\text{inf}} - T_{CF}$.

($0.25 \leq x \leq 0.7$) is characterized by the increase of the T_K temperature with x .¹⁴ This increase is evidenced by the shift of the position of the maximum in $\rho(T)$ to higher temperatures, from nearly $T_{\rho_{\max}} = 16$ K at $x=0.3$ to $T_{\rho_{\max}} = 50$ K at $x=0.8$ (see Fig. 2 and Table I). The T_K values extracted from γ_0 [using $T_K \approx 1/\gamma_0$ (Ref. 19)] coincide with those obtained from the transport measurements.

However, none of the $C_{el}(T)/T$ curves can be fitted with the predictions for a classical Kondo system. The decrease of $C_{el}(T)/T$ at low temperature as the Cu content increases (see Fig. 6) indicates a progressive reduction of the low-energy degrees of freedom. In terms of entropy gain (ΔS), it reaches one-half of the expected value ($\Delta S = R \ln 2$) for a doublet Ce ground state at 20 K. From a usual Kondo model,¹⁹ one-half of the entropy is gained at around $1.3 T_K$, which in the case of $x=0.7$ would give $T_K \approx 15$ K, whereas one observes a $T_{\rho_{\max}} = 50$ K that coincides with the T_K obtained from the $T_K \approx 1/\gamma_0$ relationship.

However, the large value of T_K (≈ 50 K), reached at intermediate concentrations, requires one to take also into account at least the first CF excited levels. A good tool for such an analysis is the study of the variation of $\rho(T)$ at high temperatures.¹⁵ Above $T_{\rho_{\max}}$, the electronic scattering involving the CF levels is observed as a broad anomaly, centered at a temperature T_{CF} , proportional to the CF splitting energy ($T_{CF} \propto 2\Delta_{CF}$).²⁰ From its broadness the hybridization strength (Γ_{CF}) of those levels with the conduction states can be estimated. For practical purposes, the analysis of the second derivative of $\rho(T)$ gives a reliable approximation of these parameters. The maximum of the Kondo scattering, $T_{\rho_{\max}}$, of the CF ground state is defined as the first minimum of $d^2\rho/dT^2$, T_{CF} at the second minimum, and T_{inf} (the inflection point) as the following zero of $d^2\rho/dT^2$, with $T_{\text{inf}} - T_{CF} \propto \Gamma_{CF}$. The respective evolution of these parameters with concentration is collected in Fig. 9. There, one has to remark on the similarity between the $T_K(x)$ values extracted from $T_{\rho_{\max}}$ and the $\Gamma_{CF}(x)$ ones, indicating that in this case the

respective hybridization strengths are nearly the same for the ground and the excited CF levels. Going back to Fig. 2, one can see that around $x=0.8$ both maxima practically come together because T_K plus Γ_{CF} approaches Δ_{CF} , smearing out the characteristics of the doublet ground state (g.s.) that controls the magnetic properties at other concentrations. The contribution of the higher CF levels could explain the discrepancy at $x=0.7$ between T_K obtained from γ_0 and T_K obtained from the position where $\Delta S(T)=1/2R \ln 2$.

A question arises here whether both extremes of concentration (i.e., CePd_2Si_2 and CeCu_2Si_2) have the same CF doublet g.s. or not. In spite of the effort done in determining the doublet g.s. of the stoichiometric compounds of this system precise knowledge of their respective eigenfunctions presents some contradictions. For example, neutron diffraction studies on CePd_2Si_2 (Ref. 21) give a second-order CF coefficient $B_0^2 = -11$ K, which as a dominant term implies the magnetic moments pointing in the direction of the c axis, while other neutron studies on the magnetic structure²² describe that compound as having the magnetic moments on the basal plane. In the other concentration limit, different studies on CeCu_2Si_2 report contradictory functions for its CF doublet g.s.^{21,23} It is striking that the same doublet was proposed for both Pd and Cu compounds when the electronic charge of those elements has opposite sign (Pd is a holelike element whereas Cu is electronlike). In our investigation we have shown that the evolution of the c -axis lattice parameter with Cu concentration is the opposite below and above 75% of concentration. This basic modification in the symmetry properties of the system is reflected in all the properties depending of the Ce ground state, suggesting a significant modification of its eigenfunction.

On the eventuality that CePd_2Si_2 and CeCu_2Si_2 have not the same CF doublet g.s., a crossover between those levels has to occur at some concentration. Such a crossing has to be looked for around $0.7 < x < 0.8$, where the widths of the ground ($\sim T_K$) and the excited ($\sim \Gamma_{CF}$) levels are comparable to Δ_{CF} .

On the rich Cu side ($x \geq 0.8$; see Fig. 7), $\gamma_0(x)$ increases from 0.2 to 0.8 J/mol K² as $x \rightarrow 1$ and T_K [taken from $T_{\rho_{\max}}(T)$] decreases down to ≈ 20 K, whereas the exponent of the $\rho_{LT}(T) \propto T^n$ dependence seems to saturate at $n \approx 2.2$. The distinct feature in this concentration range is the maximum in C_{el}/T near 4 K. This anomaly only involves a few degrees of freedom (i.e., some percent of the electronic ΔS ; see Fig. 7).

Since this maximum is also present in the $x=0.85$ sample prepared with 20% excess of transition metals, it cannot be due to the magnetic foreign phase mentioned above and has to be intrinsic. Under a magnetic field ($B=4$ T) this maximum shifts to higher temperatures and the related entropy is almost doubled, which is very unusual behavior. The shift to higher temperatures suggests a F character.

We have collected the results of the analysis of our measurements in a phase diagram (Fig. 10). The occurrence of three different regimes is certainly triggered by the nonmonotonous evolution of T_K . The increase of T_K with x for $x \leq 0.7$ and its decrease for $x \geq 0.8$ imply a corresponding behavior of the coupling parameter g between the $4f$ and the conduction electrons. The increase of g with x for $x \leq 0.7$ can easily be explained by the decrease of the volume. The

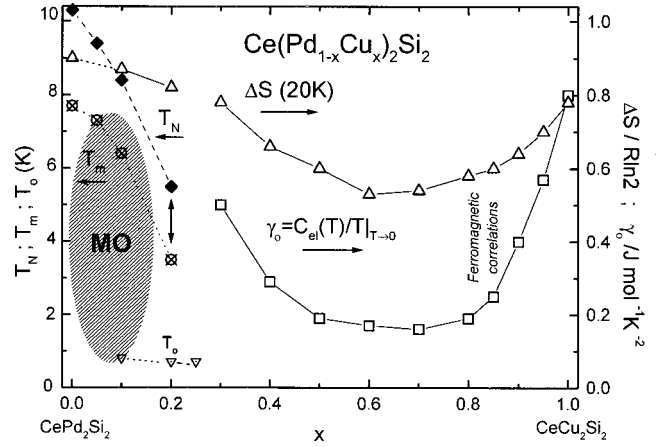


FIG. 10. Phase diagram for the low-temperature parameters: ordering temperatures (T_N , T_m , and T_0), $\gamma_0 = C_{el}(T)/T|_{T \rightarrow 0}$, and electronic entropy gain up to 20 K, $\Delta S(20 \text{ K})$.

shorter distance between Ce and its ligands leads to a larger hybridization between the $4f$ and the conduction electrons, and thus to a larger g . However, the same argument cannot be applied for $x > 0.8$, where more complex phenomena have to be involved.

The coincidence of the change in the evolution of T_K and of the c axis suggests that the origin of the anomalous behavior of g is connected with structural- and electronic-related properties. Since the nonmonotonous behavior of the c vs x is observed in both Ce- and La-based compounds, such a singular behavior has to be seen as not due to an instability of the cerium itself but instead to a general property of the Cu-Pd system.

IV. COMPARISON WITH BAND-STRUCTURE CALCULATIONS

A deeper insight into the origin of this anomalous concentration dependence is difficult to obtain, since an *a priori* calculation of the characteristic energy of the f electrons, e.g., of the Kondo temperature, is a formidably difficult task. Only very recently has such a calculation been undertaken for CeM_3 compounds by Han *et al.*²⁴ following an approach suggested by Gunnarsson *et al.*²⁵ For the CeM_3 compounds considered in Ref. 24, which have T_K differing by more than two orders of magnitude, the experimental trends were reproduced reasonably well by the calculations. It is thus interesting to see whether this approach could also reproduce the much weaker changes and the nonmonotonous behavior observed in the $\text{Ce}(\text{Pd}_{1-x}\text{Cu}_x)_2\text{Si}_2$ system and thus lead to a better understanding of this phenomenon.

We therefore investigated the electronic structure of the $\text{Ce}(\text{Pd}_{1-x}\text{Cu}_x)_2\text{Si}_2$ system using standard self-consistent band-structure calculations based on the local-density approximation (LDA). In a first step, we performed a calculation where the f electrons were treated as part of the ion core (f -core calculation). This prescription implies that the hybridization between f and band states is neglected for the calculation of the electronic states. The conduction states are determined from self-consistent scalar-relativistic calculations that include all relativistic effects except the spin-orbit interaction. The spin-orbit splittings of the Cu $3d$ and Pd $4d$

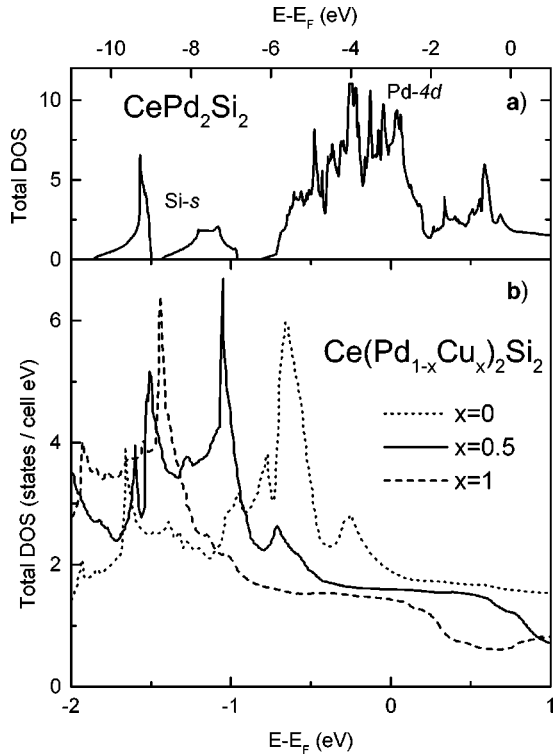


FIG. 11. Total DOS for $\text{Ce}(\text{Pd}_{1-x}\text{Cu}_x)_2\text{Si}_2$ for $x=0, 0.5,$ and 1.0 , with the Ce $4f$ electron included in the ion core (f -core calculation). The energies have been shifted so that the Fermi energy is at zero energy. (a) General overview for $x=0$. The two bands in the low-energy region are derived from the Si s states. The dominant features are the T - d bands which hybridize with Si p and T - s states near the bottom of the d bands and with Si d and T - p states near the top, respectively. (b) For $x=0$ and $x=0.5$, the DOS at the Fermi energy is increased with respect to $x=1$. For higher energies the states have predominantly Ce d character hybridized with T - p states.

states are much smaller than the corresponding bandwidths. Details of the calculation method can be found in Ref. 26.

In Fig. 11 we show the total density of states (DOS) of the conduction bands obtained from this f -core calculation. A common feature of the CeT_2X_2 ($X=\text{Si}, \text{Ge}$) compounds is the broad s - p bands [Fig. 11(a)]. In $\text{Ce}(\text{Pd}_{0.5}\text{Cu}_{0.5})_2\text{Si}_2$ and CePd_2Si_2 the Pd $4d$ states lead to an increased density $N(E_F)$ of conduction states at the Fermi level of about 1.62 states/cell eV and 1.91 states/cell eV, respectively [Fig. 11(b)]. In the related system CeCu_2Si_2 , the metal d bands are filled and, consequently, are sitting far below the Fermi energy, leading to a lower $N(E_F)$ of 1.32 states/cell eV. We checked this increase in $N(E_F)$ by performing a similar calculation for the non- f reference compounds LaCu_2Si_2 , LaPd_2Si_2 , and $\text{La}(\text{Pd}_{1-x}\text{Cu}_x)_2\text{Si}_2$ and by comparing the resulting Sommerfeld coefficient γ_{calc} with the experimental value γ_{expt} obtained from the specific heat experiments (see Table II). Both γ_{expt} and γ_{calc} show a significant increase from LaCu_2Si_2 to LaPd_2Si_2 . The calculated values are slightly lower than the experimental ones, as expected since the renormalization effects are not included in γ_{calc} . The small enhancement coefficient $m^* = \gamma_{\text{expt}}/\gamma_{\text{calc}} = 1.03$ obtained for the Cu-based compound and the slightly larger value $m^* = 1.2$ found for the Pd-based compound correspond to the

TABLE II. Comparison of the measured and calculated Sommerfeld coefficients γ_{expt} and γ_{calc} of $\text{La}(\text{Pd}_{1-x}\text{Cu}_x)_2\text{Si}_2$. m^* is defined as the ratio $\gamma_{\text{expt}}/\gamma_{\text{calc}}$. Since no specific heat data were available for $\text{La}(\text{Pd}_{0.5}\text{Cu}_{0.5})_2\text{Si}_2$, we take γ_{expt} of $\text{La}(\text{Pd}_{0.4}\text{Cu}_{0.4})_2\text{Si}_2$.

Compound	γ_{expt} [mJ/(mol K ²)]	γ_{calc} [mJ/(mol K ²)]	m^*
LaPd_2Si_2	6.2	5.3	1.20
$\text{La}(\text{Pd}_{0.5}\text{Cu}_{0.5})_2\text{Si}_2$	6.0	4.2	1.40
LaCu_2Si_2	3.5	3.4	1.03

general trends observed in transition-metal compounds, giving thus very strong support for the validity of these LDA calculations. For $\text{La}(\text{Pd}_{1-x}\text{Cu}_x)_2\text{Si}_2$, m^* is somewhat larger, but this might be due to the artificial superstructure used for the calculation of this alloy. Following the approach of Ref. 24 and Ref. 25, the hybridization strength $\Gamma_m(E_F)$ (m denotes the symmetry of the f state) determining the low-temperature properties of the Ce compounds is estimated from the f -projected density of states (f -PDOS), $\rho_{fm}^{\text{Ce}}(E)$, at the Ce site obtained from the self-consistent (LDA) band-structure calculation where the $4f$ electrons are now treated as band states:

$$\Gamma_m(E_F) = - \lim_{\eta \rightarrow 0} \text{Im} \left[\int dE \frac{\rho_{fm}^{\text{Ce}}(E)}{E_F - E - i\eta} \right]^{-1}. \quad (1)$$

This procedure seems justified since we anticipate the bare unrenormalized hybridization strengths $\Gamma_m(E_F)$ to be predominantly determined by the self-consistent potential and, concomitantly, the self-consistent electronic density distribution. The conduction electrons states in general and their coupling to the Ce $4f$ states in particular should be only weakly affected by the f correlations. The calculated hybridization strengths $N_f\Gamma = \sum_m \Gamma_m$ are listed in Table III. We get a larger value for $\text{Ce}(\text{Pd}_{0.5}\text{Cu}_{0.5})_2\text{Si}_2$ than for the two pure compounds. The calculations thus reflect nicely the non-monotonic variation of the characteristic temperature observed experimentally. The values for $N_f\Gamma$ are of comparable magnitude as those calculated for the CeM_3 system.²⁴ The influence of the metallic host can be seen from the weight of the f tails of the conduction electron states at the Ce site. The latter is reflected in the f -PDOS at the Ce site obtained when treating the f electron as part of the ion core. This conduction electron f -PDOS (see Table III) also presents a nonmonotonous variation with composition, showing a maximum for $\text{Ce}(\text{Pd}_{1-x}\text{Cu}_x)_2\text{Si}_2$. Thus the standard *ab initio* LDA band-structure calculations provide a good qualitative description for electronic properties such as the hy-

TABLE III. Hybridization strengths (a) and f -projected DOS at the Fermi level from the f -core calculation (b).

Compound	(a) [eV]	(b) [states/(eV (Ce atom))]
CePd_2Si_2	0.272	0.014
$\text{Ce}(\text{Pd}_{0.5}\text{Cu}_{0.5})_2\text{Si}_2$	0.367	0.016
CeCu_2Si_2	0.326	0.015

bridization strengths. The results can explain trends in the characteristic energies in $\text{Ce}(\text{Pd}_{1-x}\text{Cu}_x)_2\text{Si}_2$ observed in the experiments. According to these calculations the origin of the maximum of the $4f$ -energy scale in $\text{Ce}(\text{Pd}_{1-x}\text{Cu}_x)_2\text{Si}_2$ can be traced to a maximum of the conduction electron hybridization strength at the Ce site.

V. CONCLUSIONS

Our results clearly indicate the existence of three different regions in the composition dependence of the properties of $\text{Ce}(\text{Pd}_{1-x}\text{Cu}_x)_2\text{Si}_2$. In the low-concentration region ($x < 0.3$) the AF ordering temperature T_N decreases and the transition broadens with increasing x , whereas a second anomaly at $T_m \approx 0.8 T_N$ becomes more pronounced. In contrast, no evidence of magnetic order is observed in the middle concentration range ($0.3 \leq x \leq 0.7$), where the main feature is a significant increase of the Kondo temperature with increasing Cu content, from $T_K = 16$ K at $x = 0.3$ to $T_K = 40$ K at $x = 0.8$. Strong deviations from Fermi-liquid behavior in the T dependence of $\rho(T)$, $C_{el}(T)$, and $\chi(T)$ are observed in this concentration range, especially near the boundary where the magnetic order disappears.

At high Cu contents ($x > 0.7$), an anomaly involving a small part of the entropy appears at $T \approx 4$ K, whose field

dependence points to F character. T_K is rapidly decreasing in this concentration range. The nonmonotonous behavior of T_K is a unique feature of this system, contrasting the monotonous dependence observed in all other Ce-alloy systems. The change in the evolution of all the studied properties at $x = 0.8$ corresponds to a rather abrupt change in the composition dependence of the c lattice parameter in both Ce- and La-based alloys, pointing to a structural related origin of this unique behavior. The nonmonotonous $T_K(x)$ dependence is reproduced using LDA band-structure calculations, which show a maximum of the hybridization strength between conduction electrons and Ce $4f$ states for intermediate Cu concentrations.

ACKNOWLEDGMENTS

This work was partially supported by a cooperation program between the Deutscher Akademischer Austauschdienst and Alexander von Humboldt Foundation (Germany) and Fundacion Antorchas (Argentina). Partial support was also received from the ‘‘Sonderforschungsbereich 252’’ and ‘‘Proyecto de Investigación Plurianual.’’ J.G.S., M.G.B., O.T., and P.P. are affiliated with CONICET and Instituto Balseiro.

- ¹A. Loidl, A. Krimmel, G. Knopp, G. Sparn, M. Lang, C. Geibel, S. Horn, A. Grauel, F. Steglich, B. Welslau, N. Grewe, H. Nakotte, and A. P. M. F. R. de Boer, *Ann. Phys. (Leipzig)* **1**, 78 (1992).
- ²J. G. Sereni and O. Trovarelli, *J. Magn. Magn. Mater.* **140-144**, 885 (1995).
- ³A. Szytula, in *Handbook of Magnetic Materials*, edited by K. H. J. Buschow (Elsevier, New York, 1991), Vol. 6, Chap. 2.
- ⁴R. Feyerherm, A. Amato, C. Geibel, F. N. Gygax, P. Hellmann, R. H. Heffner, D. E. MacLaughlin, R. Müller-Reisener, G. J. Nieuwenhuys, A. Schenck, and F. Steglich, *Physica B* **206-207**, 596 (1995).
- ⁵P. Haen, F. Mallmann, M. J. Besnus, J. P. Kappler, F. Bourdarot, P. Burlet, and T. Fukuhara, *J. Phys. Soc. Jpn.* **65**, Suppl. B 16 (1996).
- ⁶R. Modler, M. Lang, C. Geibel, C. Schank, R. Müller-Reisener, P. Hellmann, A. Link, G. Sparn, W. Assmus, and F. Steglich, *Physica B* **206-207**, 586 (1995).
- ⁷P. Gegenwart, M. Lohmann, M. Lang, R. Helfrich, C. Langhammer, M. Köppen, C. Geibel, F. Steglich, and W. Assmus, *Physica B* **230-232**, 572 (1987).
- ⁸W. Jeitschko and M. Reehuis, *J. Phys. Chem. Solids* **48**, 667 (1987).
- ⁹R. Movshovich, T. Graf, D. Mandrus, J. D. Thompson, J. L. Smith, and Z. Fisk, *Physica B* **53**, 8241 (1996).
- ¹⁰S. R. Julian, C. Pfleiderer, F. M. Grosche, N. D. Mathur, G. J. McMullan, A. J. Diver, I. Walker, and G. Lonzarich, *J. Phys.: Condens. Matter* **8**, 9675 (1996).
- ¹¹D. Jaccard, K. Behnia, and J. Sierro, *Phys. Lett. A* **163**, 475 (1992).
- ¹²F. Steglich, B. Buschinger, P. Gegenwart, M. Lohmann, R. Helfrich, C. Langhammer, P. Hellmann, L. Donnevert, S. Thomas, A. Link, C. Geibel, M. Lang, G. Sparn, and W. Assmus, *J. Phys.: Condens. Matter* **8**, 9909 (1996).
- ¹³J. G. Sereni and J. P. Kappler, *J. Phys.: Condens. Matter* **6**, 4771 (1995).
- ¹⁴M. Weiden, O. Trovarelli, M. Gomez Berisso, R. Müller-Reisener, C. Geibel, J. G. Sereni, and F. Steglich, *Physica B* **223-224**, 229 (1996).
- ¹⁵J. G. Sereni, *Physica B* **215**, 273 (1995).
- ¹⁶R. Müller-Reisener, Ph.D. thesis, Technische Hochschule Darmstadt, Germany, 1995.
- ¹⁷J. G. Sereni, C. Geibel, M. Gomez Berisso, P. Hellmann, O. Trovarelli, and F. Steglich, *Physica B* **230-232**, 580 (1997).
- ¹⁸M. B. Maple, R. Dickey, J. Hermann, M. C. de Andrade, E. J. Freeman, D. A. Gajewski, and R. Chau, *J. Phys.: Condens. Matter* **8**, 9773 (1996).
- ¹⁹H. Desgranges and K. D. Schotte, *Phys. Lett.* **91A**, 240 (1982).
- ²⁰D. Cornut and B. Coqblin, *Phys. Rev. B* **5**, 4541, (1972).
- ²¹A. Severing, E. Holland-Moritz, B. D. Rainford, S. R. Culverhouse, and B. Frick, *Phys. Rev. B* **39**, 2557 (1989).
- ²²R. A. Steeman, E. Frikkee, R. B. Helmholtz, A. A. Menovsky, J. van den Berg, G. J. Nieuwenhuys, and J. Mydosh, *Solid State Commun.* **66**, 103 (1988).
- ²³E. A. Goremychkin and R. Osborn, *Phys. Rev. B* **47**, 14 280 (1993).
- ²⁴J. E. Han, A. Alouani, and D. L. Cox, *Phys. Rev. Lett.* **78**, 939 (1997).
- ²⁵O. Gunnarsson, O. K. Andersen, O. Jepsen, and J. Zaanen, *Phys. Rev. B* **39**, 1708 (1989).
- ²⁶G. Zwircknagl, *Adv. Phys.* **41**, 203 (1992); G. Zwircknagl (unpublished).